EUKARYOTIC CELL, June 2008, p. 1019–1028 Vol. 7, No. 6
1535-9778/08/$08.00+0 doi:10.1128/EC.00413-07

Molecular Signals in the Trafficking of *Toxoplasma gondii* Protein MIC3 to the Micronemes▽

Hiba El Hajj,[1] Julien Papoin,[1] Odile Cérède,[3] Nathalie Garcia-Réguet,[2] Martine Soête,[2] Jean-François Dubremetz,[1] and Maryse Lebrun[1]*

UMR 5235 CNRS, Université de Montpellier 2, CP 107, Place Eugène Bataillon, 34090 Montpellier, France[1]; FRE 2377 CNRS, Institut de Biologie de Lille, 1 rue du Professeur Calmette, 59021 Lille, France[2]; and UMR Université-INRA d'Immunologie Parasitaires, Faculté des Sciences Pharmaceutiques et Biologiques, 31 Avenue Monge, 37200 Tours, France[3]

Received 9 November 2007/Accepted 26 February 2008

The protozoan parasite *Toxoplasma gondii* is equipped with a sophisticated secretory apparatus, including three distinct exocytic organelles, named micronemes, rhoptries, and dense granules. We have dissected the requirements for targeting the microneme protein MIC3, a key component of *T. gondii* infection. We have shown that MIC3 is processed in a post-Golgi compartment and that the MIC3 propeptide and epidermal growth factor (EGF) modules contain microneme-targeting information. The minimal requirement for microneme delivery is defined by the propeptide plus any one of the three EGF domains. We have demonstrated that the cleavage of the propeptide, the dimerization of MIC3, and the chitin binding-like sequence, which are crucial for host cell binding and virulence, are dispensable for proper targeting. Finally, we have shown that part of MIC3 is withheld in the secretory pathway in a cell cycle-dependent manner.

The apicomplexa are a group of mostly obligate intracellular parasites that are responsible for diseases such as toxoplasmosis, malaria, neosporosis, coccidiosis, and cryptosporidiosis. Host cell invasion is a prerequisite for the establishment and maintenance of infection for these parasites, and although the range of host cell specificity can vary greatly between different apicomplexan species, the machinery they use to invade their host(s) is strikingly conserved. *Toxoplasma gondii*, the parasite responsible for congenital infections in the developing fetus and for severe neurological complications in immunocompromised individuals, is relatively easy to manipulate genetically, invades virtually all nucleated cells, and, thus, is a good model for studying motility and invasion. Host cell invasion is accompanied by the secretion of parasite proteins from two distinct secretory organelles that are associated with attachment/motility (microneme proteins [MICs]) (23, 26), parasitophorous vacuole biogenesis (rhoptry proteins) (17), and moving junction formation (cooperative role of MICs and rhoptry neck proteins) (2, 27). Exocytosis from dense granules, a third type of specialized secretory granules, occurs during and following the invasion of the host cell and is believed to take part in the maturation of the parasitophorous vacuole, although most of the GRA proteins have not yet been attributed a function (30).

The endoplasmic reticulum (ER) is the site of synthesis and the processing of proteins destined for secretion; thus, almost all secretory proteins contain a signal peptide. Most of protein sorting takes place either in the *trans*-Golgi network (TGN) (or its equivalent) or in immature secretory vesicles beyond the TGN. In *T. gondii*, soluble foreign reporter proteins, lacking targeting information, are delivered to the parasitophorous vacuole via the dense granules, which are the default route for secreted proteins (22). Similarly to other eukaryotic sorting mechanisms, a system of tyrosine-dependent signals exists in *T. gondii* that allows for the specific targeting of transmembrane proteins to the rhoptries or micronemes (13, 21, 34). Soluble MICs, which do not possess a cytoplasmic tail accessible to the cytosolic machinery, are escorted by transmembrane MICs with which they are tightly associated (34). These complexes also seem to play a functional role, as these proteins would act in concert and not individually (26).

MIC3 is a 90-kDa dimeric soluble protein containing a chitin binding-like domain (CBL), three tandemly repeated epidermal growth factor-like domains (EGF2, EGF3, and EGF4), and two less-conserved EGF domains that overlap with the others (EGF1 and EGF5) (18). MIC3 possesses binding activity to host cell surfaces (18) and recently was shown to be involved in the virulence of *Toxoplasma* in a mouse model of infection (10). The chitin binding domain was first identified in wheat germ agglutinin and then in a large number of other chitin binding proteins of plant origin. In MIC3, the CBL has been shown to be required for binding to host cells, while the EGFs modulate this binding (9). The structure of these two types of domains is disulfide bond dependent. The dimerization domain of MIC3 is located in the 66 carboxy-terminal amino acid residues (9) and is required for host cell binding. MIC3 is synthesized as a precursor that is proteolytically processed (1), such processing being a prerequisite to the expression of the binding function of the protein (9). MIC3 has been shown to interact with the transmembrane MIC8, suggesting that MIC8 functions as an escort for MIC3 (29). However, recent results have shown that in the absence of MIC8, MIC3 was perfectly localized to the micronemes (M. Meissner, personal communication).

Here, we have investigated the domains that are both necessary and sufficient to target the protein MIC3 to the mi-

* Corresponding author. Mailing address: UMR 5235 CNRS, Université de Montpellier 2, CP 107, Place Eugène Bataillon, 34090 Montpellier, France. Phone: 33 467 143 455. Fax: 33 467 144 286. E-mail: maryse.lebrun@univ-montp2.fr.

▽ Published ahead of print on 4 April 2008.

cronemes and showed that any of the EGF domains, along with the propeptide domain, fulfill these criteria.

MATERIALS AND METHODS

Host cell and parasite cultures and antibodies (Abs). *T. gondii* RH *hxgprt* (RHΔhx), deleted for hypoxanthine guanine phosphoribosyl transferase (HXGPRT) (16), and a *mic3* KO (10) were used throughout the study. All parasites were maintained by serial passage in primary human foreskin fibroblasts grown in Dulbecco's modified essential medium (DMEM) (Gibco-BRL) supplemented with 10% fetal calf serum (FCS) and 2 mM glutamine.

The Abs used were the following: monoclonal Abs (MAbs) against MIC3 (T4 2F3 and T8 2C10), rabbit anti-MIC3 (18) and mouse anti-MIC3 propeptide (9), rabbit anti-pro-M2AP (20), rabbit anti-IMC1 (28), anti-TY tag (5), rabbit anti-GRA3 (6), rabbit anti-MIC6 (34), and rabbit anti-MIC4 (34).

Plasmid constructs. The primers used for constructions were the following: ML11, 5′-GCACAATTGAGATCTAAAATGCGAGGCGGGACGTCC-3′; ML12, 5′-TGCTATGCATCCTAGGTCTGCTTAATTTTCTCACACGTCAC-3′; ML15, 5′-TGCTATGCATTCCTAGGCTGCTTAATTTTCTCACACGTCAC-3′; ML22, 5′-GCACAATTCCCTAGGTTTCTCAGCCAGCGTGACTTC-3′; ML25, 5′-GCACAATTGCCTAGGGCAGTCTCCTCCATAGCTTTTGTC-3′; ML26, 5′-GCACAATTGCCTAGGAGGATCCTCGGAGCAAGTCAA-3′; ML27, 5′-GCACAATTGCCTAGGTCCAGTCCTCTTGCATCCTTG-3′; ML64, 5′-CGCGATATCCTCCTGCTTGCTGGGGGATTG-3′; ML65, 5′-GGGGATATCAGCTGTGAAAAGCAGGGCCATCGG-3′; ML124, 5′-CGCGATATCTGTTCAAAAAGAGGGAACGCG-3′; and ML128, 5′-CGCGATATCTGTCATGCCTTCAGGGAGAAC-3′.

Plasmids pML1, pML2, pML3, pML4, pML5, pML6, pML7, pML8, and pML9 were designed to express MIC3ΔPro, SSPL, SSPLE2, SSPLE23, MIC3ΔCBL, SSPE2, SSPE3, SSPE4, and SSP-CBL-$AA_{294-359}$ proteins, respectively, in *mic3* KO parasites.

Plasmid pML1 was based on plasmid pM3MIC3ty (10), in which the *MIC3* open reading frame was replaced by a *MIC3* sequence lacking the propeptide coding sequence. The latter was PCR amplified from pSS-MIC3 (9) with primers ML11/ML15 and cloned into BglII and AvrII sites of pM3MIC3ty. BglII and AvrII sites were present downstream of the ATG start codon of MIC3 and the ty sequence of pM3MIC3ty, respectively.

Plasmids pML2, pML3, and pML4 were constructed in pM3MIC3ty by PCR amplification from pBlueMIC3 (18) with primers ML22/ML25, ML22/ML26, and ML22/ML27, respectively, digestion of the PCR fragments by BglII and AvrII, and being cloned in pM3MIC3ty digested by BglII and AvrII to replace the *MIC3* open reading frame.

Plasmids pML5 and pML6 were constructed by PCR amplification of pM3MIC3ty and pML3 with primers ML64/ML65 to create the deletion of the CBL domain. The ML64 and ML65 primers were designed to add the restriction site EcoRV at the 5′ end upon PCR amplification. The template plasmids were eliminated by digestion with DpnI, and the PCR fragments were digested with EcoRV and finally recircularized by ligation.

Plasmid pML7 was constructed by the PCR amplification of pML4 with primers ML64/ML124 to create the deletion of the CBL domain plus EGF2 sequences and was recircularized as described for pML5 and pML6.

Plasmid pML8 was constructed by the PCR amplification of the EGF4 sequence from pBlueMIC3 with primers ML22/ML128 and being cloned into EcoRV and AvrII sites of pML6 to replace EGF2 with EGF4.

Plasmid pML9 was constructed by an in-frame deletion of the EcoRI fragment of pM3MIC3ty.

QuikChange (Stratagene), a PCR-based site-directed mutagenesis system, was used to introduce mutations W126 and F128 into the *MIC3* gene, as described previously (10).

All constructs were verified by sequencing.

Transfection and selection. Transfections of parasites were conducted as described previously (10). In that work, the complementation of the *mic3* KO clone by MIC3ty had been obtained by cotransfection using 100 μg of pM3MIC3ty and 10 μg of pTUB/pCAT plasmids. The same procedure was used for all other constructs bearing targeted deletions. After overnight growth, transfectants were selected with 20 μM chloramphenicol for three passages before being cloned by limiting dilution under drug selection. After the clones were expanded, transgenic parasites were identified by immunofluorescence assay (IFA) with anti-Ty MAbs (5).

Immunolocalization experiments. For IFA on intracellular parasites, cell monolayers were washed in phosphate-buffered saline (PBS) and fixed in 4% paraformaldehyde for 20 min. After three washes, cells were permeabilized either with 0.1% Triton X-100 or with 0.05% saponin in PBS for 10 min, blocked with 10% fetal bovine serum in PBS (PFBS) for 30 min, incubated with primary Abs (MAb T4 2F3, T8 2C10, or anti-ty1; mouse serum anti-MIC3 propeptide; or rabbit serum anti-IMC1, anti-GRA3, anti-MIC6, anti-MIC4, anti-MIC3 or anti-pro-M2AP), diluted in 2% PFBS, washed, and then incubated with secondary antibody (fluorescein isothiocyanate goat anti-mouse and/or Texas Red goat anti-rabbit; Sigma). IFA on invading parasites was performed as described previously (27).

The coverslips were mounted onto microscope slides using Immunomount (Calbiochem). All observations were performed on a Leica DMRA2 microscope equipped for epifluorescence, and images were recorded with a Coolsnap charge-coupled display camera (Photometrics, Tucson, AZ). Adobe Photoshop (Adobe Systems, Mountain View, CA) was used for image processing. When required, matching pairs of images were recorded with the same exposure time and processed identically.

SDS-PAGE and Western blotting. Sodium dodecyl sulfate-polyacrylamide gel electrophoresis (SDS-PAGE) was performed according to Laemmli (25). Freshly released tachyzoites were boiled in SDS sample buffer with (reduced) or without (nonreduced) 0.1 M dithiothreitol (DTT) and separated on 10 or 15% polyacrylamide gels. Proteins were transferred to nitrocellulose membranes. Western blots were probed with MAb anti-MIC3 T4 2F3 or T8 2C10 (1:400), MAb anti-Ty (1:400), or mouse anti-MIC3 propeptide (1:500), followed by goat anti-mouse or goat anti-rabbit immunoglobulin G alkaline phosphatase conjugates (1:500) (Sigma).

Metabolic labeling and immunoprecipitation. A 75-cm^2 monolayer of human foreskin fibroblast cells that had been infected 24 h earlier with 1×10^7 tachyzoites was washed with methionine- and cysteine-free DMEM (Gibco) and incubated for 30 min at 37°C in the same medium supplemented with 5% dialyzed FCS and containing 50 μCi/ml of a mixture of [^{35}S]methionine and [^{35}S]cysteine (Translabel; NEN) with or without 5 μg/ml brefeldin A (BFA) (Sigma). The infected monolayer was washed with medium, followed by either immediate lysis (in 0.5% NP-40, 50 mM Tris-HCl, pH 8.3, 100 mM NaCl, 1 mM EDTA) or chase in complete culture medium at 37°C for 1 or 2 h before lysis. Immunosorbent production and immunosorption procedures were performed as described previously (1). Briefly, T4 2F3 immunoglobulins were purified from ascitic fluid and coupled to CNBr-activated Sepharose 4B (Pharmacia). Labeled lysates were incubated with the immunosorbents for 16 h at 4°C under gentle agitation and were washed five times with a buffer containing 1 M NaCl, 0.5% NP-40 in 50 mM Tris-HCl, pH 8.3. Elution then was performed for 5 min at 95°C with electrophoresis sample buffer.

Electron microscopy. Infected cells were fixed with 4% paraformaldehyde–0.05% glutaraldehyde in 0.2 M sodium phosphate buffer for 90 min, washed in PBS–10% FCS (PBSFCS), and infused in 2.3 M sucrose containing 10% polyvinylpyrrolidone before being frozen in liquid nitrogen. Sections were obtained on a Leica Ultracut equipped with a FCS cryoattachment operating at −100°C. Sections were floated successively on PBSFCS, anti-Ty MAb ascites diluted 1:40 in PBSFCS, rabbit anti-mouse serum diluted 1:400 in PBSFCS, and 10-nm protein A-gold diluted in PBS to optical density at 525 nm of 0.05, with five 3-min washes in PBS between each step. Sections then were embedded in 2% methylcellulose–uranyl acetate (0.4%) and observed with a Zeiss EM10 electron microscope.

RESULTS

MIC3 is retained in the secretory pathway in recently replicated parasites. We first assessed the cellular localization of MIC3 in intracellularly replicating *T. gondii* tachyzoites. In contrast to other MIC proteins analyzed, MIC3 showed a peculiar labeling pattern upon IFA. Indeed, MIC3 labeling was not always restricted to micronemes but also could extend posteriorly (Fig. 1A). This labeling was observed with both anti-MIC3 MAbs and with polyclonal anti-MIC3 in strain RH (illustrated here) and in other *T. gondii* strains (data not shown) but not in the *mic3* KO strain (data not shown). In some cases, we detected a subcellular compartment typically resembling the Golgi apparatus (32) (Fig. 1A). In others, an intense nuclear envelope and posterior staining was observed that was typical of ER labeling (Fig. 1C) (19). Interestingly, this labeling was not observed in all vacuoles. In order to test for a possible stage specificity of this ER-Golgi complex MIC3 staining, we performed coimmunostaining with an anti-IMC1

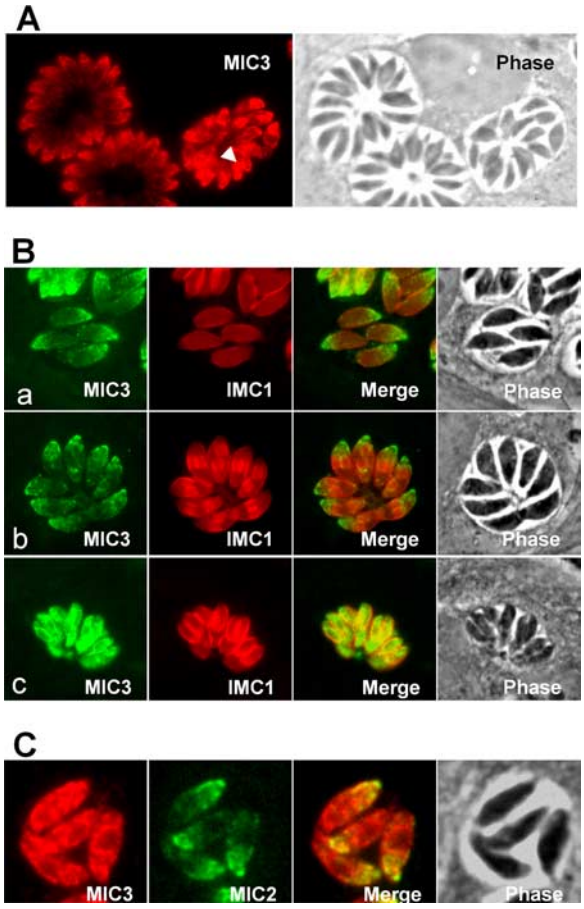

FIG. 1. Cell cycle-regulated expression of MIC3 in strain RH. (A) Three vacuoles in the same field stained with anti-MIC3 are presented here to illustrate the cycle-dependent retention of MIC3 in the early compartments of the secretory pathway. The IFA of intracellular tachyzoites with polyclonal anti-MIC3 (red) shows apical punctate fluorescence that is typical of microneme staining (vacuoles on the left side) or ER-Golgi complex staining (arrowhead; vacuoles on the right side). (B) Dual-label immunofluorescence microscopy on intracellular parasites with MAb T4 2F3 and anti-IMC1 Abs. Late dividing stages (c) show the ER-Golgi complex retention of MIC3. (C) Intracellular parasites stained with rabbit anti-MIC3 and MAb anti-MIC2 showing that ER-Golgi complex retention is restricted to MIC3.

serum, which allows the visualization of the inner membrane complex of daughter cells during endodyogeny (28). The strong perinuclear labeling was not associated with parasites at early stages of endodyogeny but was observed only at a late stage of duplication (separating parasites) and in thin newly replicated parasites (Fig. 1B, row c). This suggested that dividing parasites express a large amount of MIC3 that is not immediately targeted to micronemes and is retained into the secretory pathway. This was not observed for MIC2 (Fig. 1C), MIC1, MIC8, or AMA1 (data not shown), which are other major microneme proteins, indicating that stage-specific retention is not a general feature of microneme protein trafficking.

Processing of MIC3 occurs in a post-Golgi compartment. Previous studies have shown that MIC3 was processed between 15 min and 1 h after synthesis (1). To investigate whether this proteolytic processing occurs beyond the ER, we inhibited exit from the ER with BFA. This drug induces a disassembly of the proximal part of the Golgi compartment, resulting in a redistribution of *cis*-, medial-, and *trans*-Golgi resident enzymes back into the ER, and blocks forward transport to the TGN (24). Tachyzoites were pulse labeled for 30 min with [^{35}S]methionine and [^{35}S]cysteine and then chased with excess cold methionine and cysteine in the presence or absence of BFA. MIC3 was immunoprecipitated either before or after the chase with a specific antibody (Fig. 2A). As expected, in the absence of drug, a large part of MIC3 was processed from a proprotein to a mature protein within 60 min (Fig. 2A). In the presence of BFA, pro-MIC3 remained the only species at the end of the chase (Fig. 2A). This block was reversible, since an additional chase of 1 h without drug allowed the partial processing of MIC3. This result shows that MIC3 processing is a rapid event that occurs in a post-medial-Golgi compartment.

To define more precisely the MIC3 processing compartment, we searched for the distribution of pro-MIC3 by IFA with a specific anti-propeptide antiserum (9). Unprocessed MIC3 staining was localized to perinuclear areas (ER and/or Golgi compartment) (Fig. 2B). We could not detect unprocessed MIC3 in micronemes. As mentioned previously, the labeling of perinuclear areas (ER and/or Golgi compartment) with the anti-propeptide antiserum was restricted to dividing or thin newly replicated parasites, strongly suggesting that the protein retained in the secretory pathway is the MIC3 precursor.

All of these results are consistent with the NH_2-terminal processing of MIC3 occurring after leaving the Golgi compartment.

MIC3 synthesis is slightly shifted compared to that of M2AP, another microneme protein. We then sought to compare the pattern of synthesis of MIC3 to that of M2AP, which is another microneme protein containing a propeptide that is cleaved with kinetics similar to those of pro-MIC3 (33) in the post-Golgi-endosome-like compartment (20). Since maturation of MICs occurs with rapid kinetics (8), detection using anti-pro-MIC Abs that specifically label immature MICs faithfully reflects the timing of MIC protein synthesis. We thus performed simultaneous IFA of pro-MIC3 and pro-M2AP.

As expected, pro-M2AP was seen in apical vesicles that have been described as being mainly endosome-like compartments (20) (Fig. 2C). This labeling was almost always associated with the pro-MIC3 staining (93% of the positive pro-M2AP vacuoles were also pro-MIC3 positive) (Fig. 2C, rows b and c), indicating that MIC3 and M2AP are synthesized almost simultaneously. The thin shape of these parasites in phase contrast indicated that they corresponded to newly separated parasites. While pro-M2AP mainly occupied the endosome-like compartments, pro-MIC3 was detected either in the ER-Golgi complex (55.9%) or, as is the case for pro-M2AP, in endosome-like compartments (44.1%). There were no detectable morphological differences between these two populations in phase contrast. Some pro-M2AP staining also was observed in the absence of pro-MIC3 (Fig. 2C, row d). This corresponded to 8% of the pro-M2AP-positive vacuoles and always was associated with fully separated parasites (thick-shaped parasites). In addition, a prominent ER staining of MIC3 also was detected in pro-M2AP-negative parasites (Fig. 2C, row a) (9% of the pro-MIC3 positive vacuoles), and in this case it was always associated with dividing but not fully separated para-

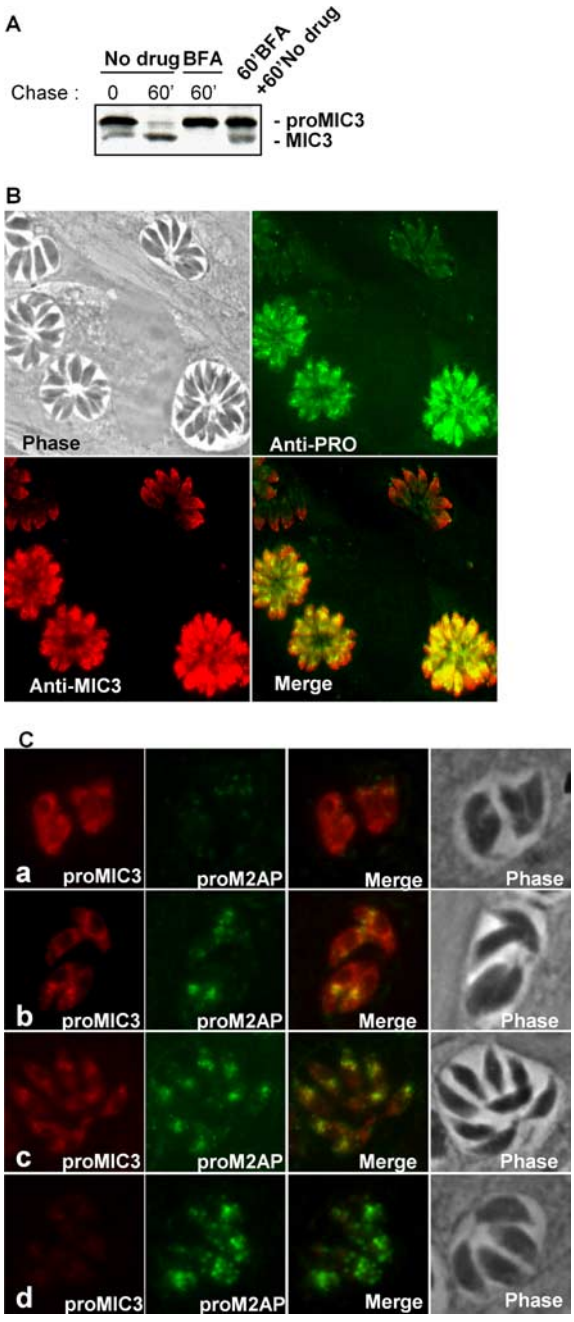

FIG. 2. Proteolytic processing of MIC3 occurs beyond the Golgi compartment and prior to reaching the mature micronemes. (A) Pulse-chase metabolic labeling followed by the immunopurification of MIC3 was performed on tachyzoites chased in the presence or absence of BFA, and the products were analyzed by SDS-PAGE in reduced conditions. Lane 1 corresponds to a 15-min pulse without chase; lanes 2 and 3 correspond to 1 h of chase in the absence or presence of drug, respectively; and lane 4 corresponds to 1 h of chase with drug followed by 1 h without drug. (B) IFA of intracellular tachyzoites with anti-propeptide-specific serum. The anti-propeptide serum exclusively labels MIC3 retained in the secretory pathway. (C) Dual IFA with mouse anti-pro-MIC3 and rabbit anti-pro-M2AP Abs. Note that in the images in row a, the parasites on the left are at a very early stage of splitting and do not express any pro-M2AP but do express a large amount of ER-localized pro-MIC3, in contrast to parasites on the right, which are separating and show some dots of pro-M2AP staining. Later stages of splitting show the simultaneous labeling of both propeptides, either partly (b) or fully (c) colocalized, or stages in which pro-MIC3 is absent (d).

sites. Taken together, these results indicated that MIC3 synthesis mainly coincides with that of M2AP, with that of MIC3 starting first.

The propeptide of MIC3 is essential for proper sorting to micronemes. We then addressed the sequence requirements for targeting MIC3 to micronemes. Previous works have shown that the propeptide of MIC3 alone does not contain a microneme-targeting signal, as a chimera fusing the MIC3 signal peptide plus propeptide to green fluorescent protein (GFP) resulted in the secretion of the reporter into the parasitophorous vacuole (36). However, whether the propeptide is necessary for the proper sorting of MIC3 to micronemes had not been investigated. To address this question, we have expressed MIC3 lacking the propeptide (MIC3ΔPro) driven by the *mic3* promoter in *mic3* KO parasites. The propeptide starts after the signal peptide at position 27 and is cleaved between glutamine at position 66 and serine at position 67 in the MIC3 sequence SSVQ/SPSK (P4-P4′ residues) (18). We constructed a plasmid encoding the MIC3 sequence deleted of amino acids 27 to 66 in frame with a C-terminal sequence coding for a Ty epitope, and this plasmid was transfected into *mic3* KO parasites to yield the *MIC3ΔPro* cell line. Transgenic parasites expressing the Ty-tagged full-length MIC3 in the *mic3* KO background (*MIC3* cell line; plasmid pMIC3-MIC3) were used as controls (10).

Western blot analysis of MIC3ΔPro using the anti-Ty tag (Fig. 3A) or anti-MIC3 (not shown) MAbs demonstrated that the mutated protein migrated at the size expected for a dimer under nonreducing conditions and for a monomer under reducing conditions. This result confirmed that the propeptide is not essential for MIC3 dimerization, as shown previously in an heterologous expression system (9). As expected, no signal was detected with anti-MIC3 propeptide serum on both *mic3* KO and *mic3* KO complemented with MIC3ΔPro (Fig. 3B), and the size of the mature MIC3 was identical to that of MIC3ΔPro (Fig. 3A). Upon IFA analysis with anti-Ty tag and differential permeabilization with either Triton X-100, which allows intraparasite detection, or saponin, which restricts detection to the parasitophorous vacuole (PV) space, we showed that MIC3ΔPro was routed to the PV, unlike the wild-type-like expression of MIC3ty in *mic3* KO, which was targeted to micronemes (Fig. 3C and 4A). The presence of MIC3ΔPro in the vacuolar space was confirmed by colocalization with GRA3, a natural resident of this compartment (Fig. 3C). This mistargeting presumably occurs via the dense granules, as evidenced by the bilateral delivery in the nascent PV (Fig. 3C, final row). In this mutant, MIC8 was correctly targeted to micronemes.

We have previously shown that MIC3 propeptide is a *cis*-acting inhibitor of CBL function (9), and we suggested that the propeptide prevented the inappropriate association of MIC3 with other parasite proteins, in particular, glycosylated proteins transiting in the ER-Golgi complex. We then analyzed if MIC3ΔPro mistargeting was a consequence of latching onto glycosylated proteins, such as a GRA protein (GRA2, GRA4, or GRA6), for delivery to the PV. To address this question, we tested if MIC3ΔPro interacted with GRA2, GRA4, and GRA6, by coimmunopurification. Western blot analysis did not show any such interaction (data not shown). Since it is unclear what specific carbohydrate moiety the MIC3 CBL binds to, one cannot predict which glycoproteins are recog-

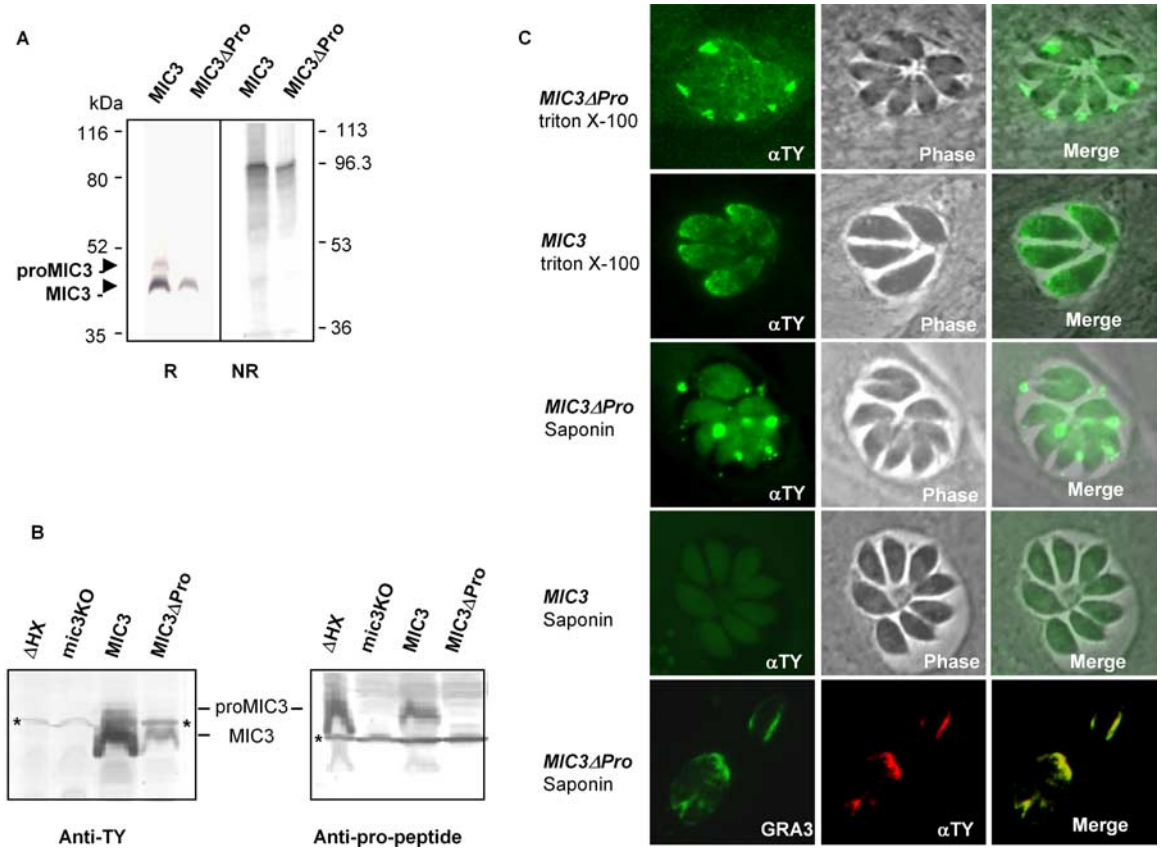

FIG. 3. Propeptide of MIC3 is necessary for MIC3 targeting to micronemes. (A) Western blot analysis in reduced (R) and nonreduced (NR) conditions of tachyzoite lysates corresponding to *mic3* KO complemented with Ty-tagged wild-type MIC3 (*MIC3* parasites) or MIC3ΔPro (*MIC3ΔPro* parasites) and probed with MAb anti-Ty (αTY); MIC3ΔPro is dimeric. Note that the immature form of MIC3ty is detected only in the reduced condition. Molecular mass standards are indicated. (B) Western blot analysis in the reduced condition of ΔHX (wild type), *mic3* KO, and *mic3* KO complemented with MIC3ty or MIC3ΔPro. The anti-propeptide serum labeled a single band in ΔHX and in *MIC3*. Anti-Ty MAb labeled a single band in *MIC3ΔPro*. In *MIC3*, it labeled the mature form of MIC3ty and faintly labeled the small amount of immature MIC3ty. Unspecific labeling is indicated by asterisks. (C) MIC3ΔPro is mistargeted and accumulates in the parasitophorous vacuole. *MIC3*- and *MIC3ΔPro*-infected cells were fixed and then permeabilized either with Triton X-100, which optimizes the staining of organelles within the parasite, or with 0.05% saponin, which allows the selective detection of proteins secreted in the parasitophorous vacuole. In contrast to MIC3ty, MIC3ΔPro was not detected in micronemes but accumulated in the parasitophorous vacuole. The bottom panel shows the perfect colocalization of MIC3ΔPro with GRA3 in the parasitophorous vacuole.

nized by the MIC3 CBL. Therefore, we then expressed a MIC3ΔPro construct in which the CBL domain of MIC3 had lost adhesive function by the single replacement of W126 or Y128, two amino acids critical for the binding properties of the CBL domain (9), with alanine. Upon IFA analysis with anti-Ty, we showed that both MIC3ΔProW126A and MIC3ΔProY128A were routed to the same parasitophorous vacuole space as MIC3ΔPro, demonstrating that the mistargeting of MIC3ΔPro to the PV probably was due to the loss of the targeting information contained in the prosequence and not to a consequence of dysregulated CBL function.

Taken together, these results showed that in the absence of a propeptide, MIC3 is delivered to the PV, the default route for soluble proteins (22), demonstrating that the propeptide of MIC3 contains targeting information for microneme delivery.

In addition to the propeptide, a single EGF domain is sufficient for MIC3 to reach the micronemes. Since the propeptide of MIC3 is necessary but not sufficient to address the protein to micronemes, we searched for the minimal sequence needed for the proper sorting of MIC3. We thus generated new constructs lacking either the EGF-like domains or the CBL domain, which were stably transfected in the *mic3* KO background. All constructs contained the MIC3 signal peptide and the propeptide and were fused at their C-terminal ends to the Ty epitope. Proteins were localized in the parasites by IFA with an anti-Ty MAb. Schematic drawings of mutated proteins and of their localization in tachyzoites are shown in Fig. 4A. In order to avoid mistargeting due to improper disulfide bridge bonding, deletions have been performed to preserve the structural features of MIC3 domains, taking into account the molecular modeling predictions of the EGF-like and CBL domains (3).

The shortest construct containing the N-terminal signal peptide, the propeptide, and the CBL domain (SSP-CBL) was first transfected in *mic3* KO parasites. An analysis of *mic3* KO parasites expressing SSP-CBL showed a faint signal in vesicular structures located on both sides of the nucleus, but this signal was absent in more than half of the parasites, suggesting

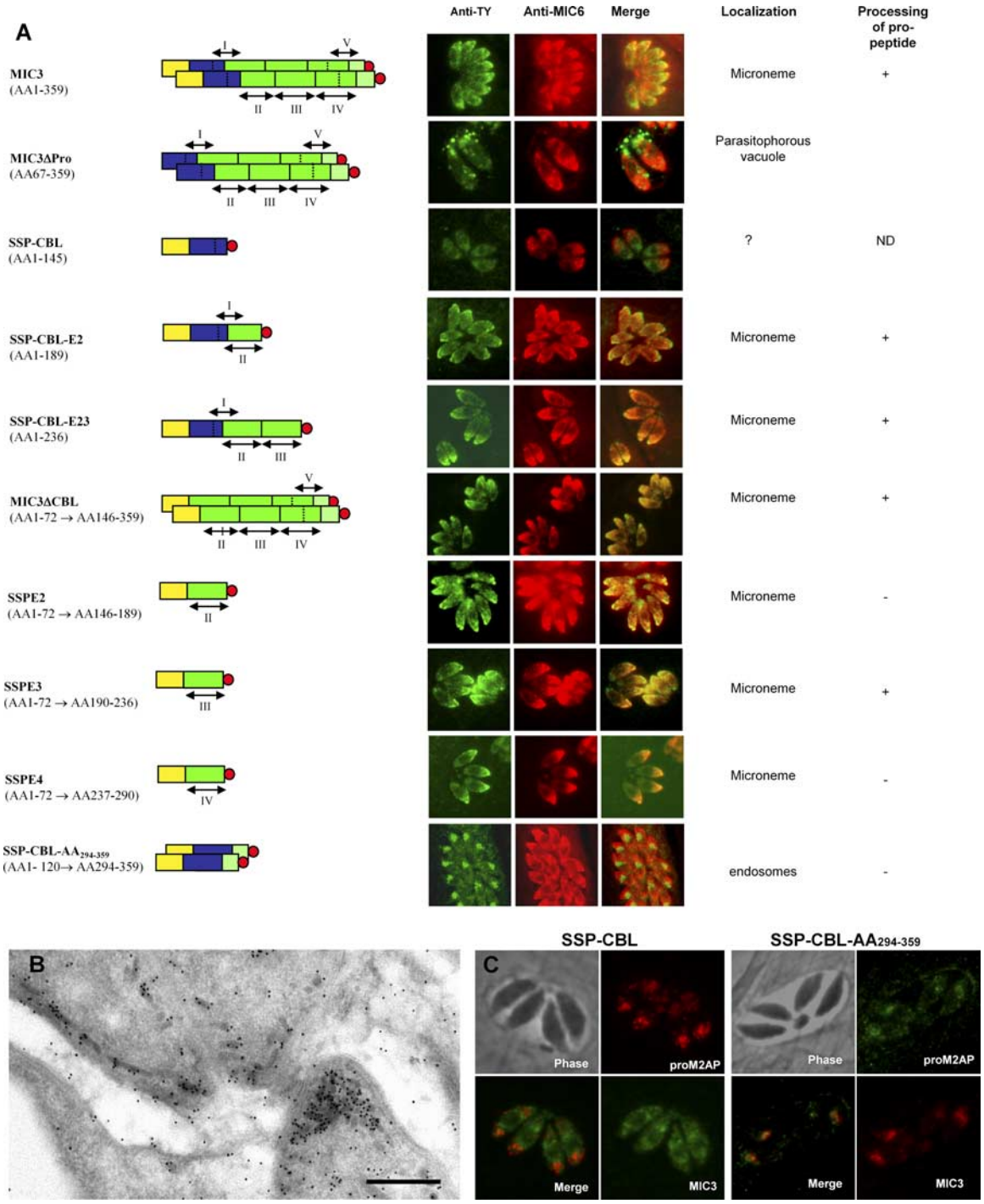

FIG. 4. (A) Schematic drawing of the MIC3 constructs and IFA of the corresponding mutants. The color code is yellow for propeptide, blue for the CBL domain, and green for the three tandemly repeated EGF domains (labeled II, III, and IV). EGF domains I and V overlap with other domains. The C-terminal stretch ($AA_{294-359}$) is represented by a dotted green area. The Ty epitope tag is indicated by a red dot. The mono- or dimeric status of the constructs also is depicted. IFAs were performed with MAb anti-Ty and rabbit anti-MIC6 Abs on intracellular parasites permeabilized with Triton X-100. The propeptide processing data also are reported (see Fig. 5B). (B) Immunolocalization with MAb anti-Ty on ultrathin cryosections of *mic3* KO tachyzoites expressing the SSPE2 construct. The protein is found essentially in micronemes (bar, 0.5 μm). (C) Dual IFA of intracellular SSP-CBL and SSP-CBL-$AA_{294-359}$ parasites. SSP-CBL was labeled with anti-Ty MAb and anti-pro-M2AP Abs. SSP-CBL-$AA_{294-359}$ was labeled with anti-MIC3 (T82C10 MAb) and anti-pro-M2AP. Colocalization is obtained only when the dimerization domain is present. ND, not detected.

that the protein was degraded. SSP-CBL was never targeted to the micronemes, as evidenced by the absence of colocalization with the microneme protein MIC8 (Fig. 4A). To better define these compartments, we used the pro-M2AP marker and showed only a partial colocalization between pro-M2AP and SSP-CBL, with pro-M2AP being located mostly in vesicles anterior to SSP-CBL.

When the EGF2 domain was added to this construct to give

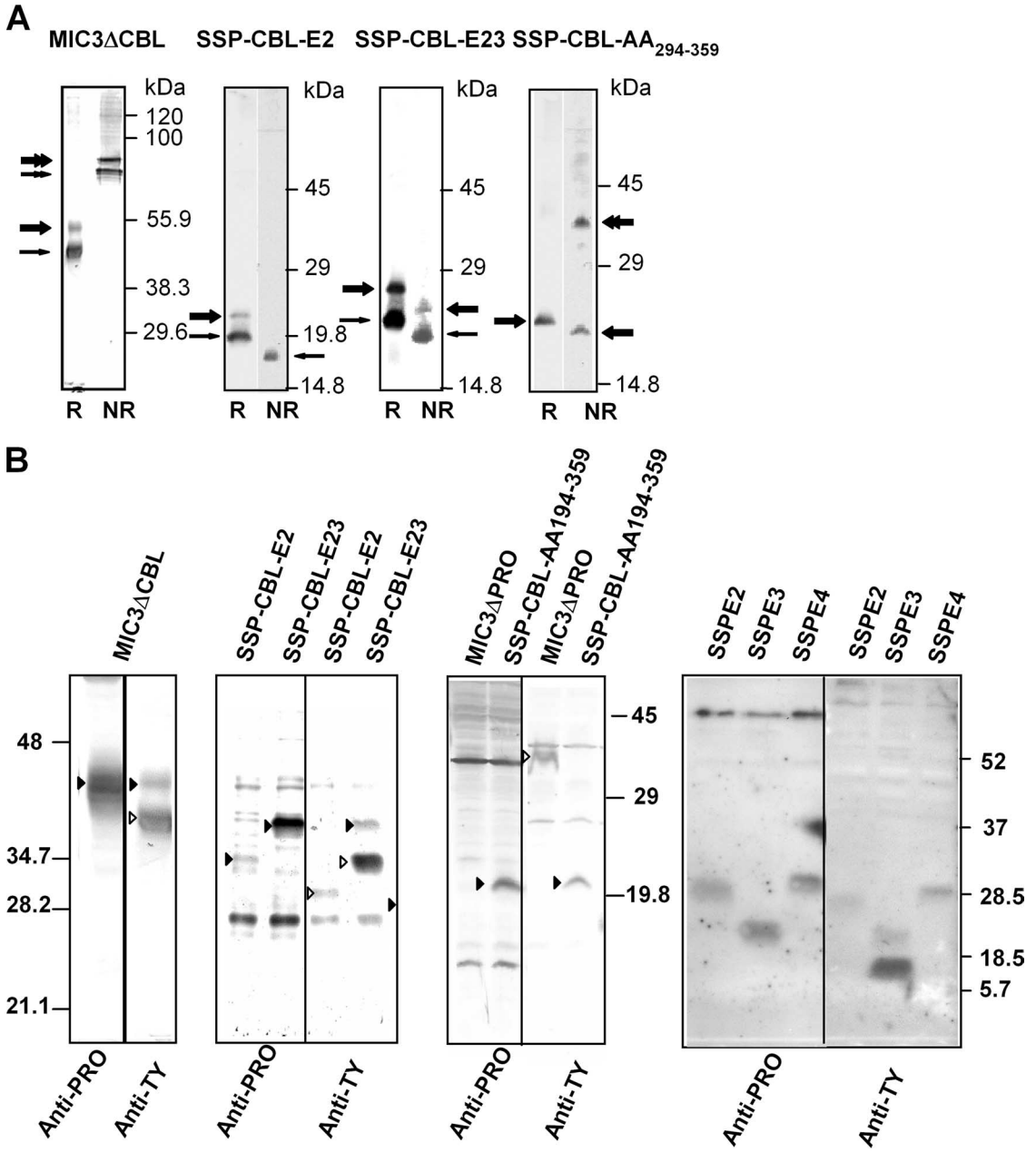

FIG. 5. Dimerization domain and the proteolytic processing of MIC3 constructs are dispensable for microneme targeting. (A) Dimerization status of MIC3 constructs. Lysates of the MIC3 recombinant parasites were separated by SDS-PAGE in reduced (R) or unreduced conditions (NR), and Western blots were probed with anti-Ty MAb. The immature and mature forms of MIC3 are indicated by thick and thin arrows, respectively. The dimers are indicated by double arrows. The migration pattern of molecular mass standards is indicated. (B) Lysates of MIC3 constructs expressing parasites were separated by SDS-PAGE in the reduced condition and probed with anti-Ty or anti-proMIC3 serum. Solid arrows point at immature proteins, and white arrows point at processed products. The anti-Ty MAb reacts with both mature and immature forms of the recombinant proteins, whereas the anti-propeptide reveals exclusively immature proteins. MIC3ΔCBL, SSP-CBL-E2, SSP-CBL-E23, and SSPE3 were correctly processed, whereas SSPE2, SSPE4, and SSPCBL-$AA_{294\text{-}359}$ were not.

SSP-CBL-E2, the protein was correctly targeted to micronemes, showing the importance of the EGF2 domain in traffic (Fig. 4A). Similarly, a construct containing EGF2 plus EGF3 (SSP-CBL-E23) was correctly addressed to micronemes. However, a synergistic role for the CBL domain together with EGF was not excluded. Therefore, we generated a construct designed to express the MIC3 protein lacking the CBL domain (MIC3ΔCBL). In order to maintain the cleavage of the propeptide, the first six amino acids of the CBL domain, which correspond to residues P1′ to P6′ of the cleavage site, were retained in the construct. As expected, immunoblot analyses showed that MIC3ΔCBL was correctly dimerized and processed (Fig. 5). Upon IFA analysis, we observed a localization of MIC3ΔCBL to micronemes (Fig. 4A), demonstrating that

the CBL domain is dispensable for MIC3 trafficking to micronemes.

To assess if either one of the EGF domains was sufficient for micronemal targeting, we then deleted the CBL domain in SSP-CBL-E2 to create SSPE2, and we showed by IFA that the construct indeed was also targeted apically (Fig. 4A). The accumulation in micronemes was confirmed by immunoelectron microscopy (Fig. 4B). Finally, we replaced EGF2 with the EGF3 or EGF4 domain to create SSPE3 and SSPE4, respectively, and showed that EGF2 could be replaced by either of the other EGF-like domains.

The last construct featured a deletion of tandemly repeated EGF2, EGF3, and EGF4 to generate SSPCBL-$AA_{294\text{-}359}$. SSP-CBL-$AA_{294\text{-}359}$ localized to the apical area of parasites, which was distinct from microneme staining (Fig. 4A) and reminiscent of the pro-M2AP pattern. To further investigate the location of this mutant, we performed dual immunofluorescence labeling of SSP-CBL-$AA_{294\text{-}359}$ with anti-pro-M2AP Abs (Fig. 4D). The distribution of SSP-CBL-$AA_{294\text{-}359}$ coincided with pro-M2AP, indicating that SSP-CBL-$AA_{294\text{-}359}$ traffics through the TGN and is retained in endosome-like structures. An IFA analysis of this mutant with the anti-pro-MIC3 serum (data not shown) and by Western blotting with anti-pro-MIC3 and anti-Ty (Fig. 5B) clearly indicated that the protein was not processed, showing that the processing of MIC3 occurs after leaving the endosomes.

Taken together, our results showed that EGF domains also participate in MIC3 targeting and that the propeptide plus any one of the three successive EGF-like domains is the minimal requirement for MIC3 targeting to micronemes.

The dimerization of MIC3 is dispensable for MIC3 trafficking to micronemes. To investigate the importance of MIC3 dimerization in targeting to micronemes, we performed Western blot analyses of the chimeric MIC3 proteins in reduced and nonreduced conditions using MAb anti-Ty (Fig. 5A). SSPE2, SSPE3, and SSPE4 were poorly expressed and were detected only in reduced conditions (data not shown); therefore, the dimerization status of these proteins could not be analyzed.

Western blot analysis of MIC3ΔCBL using anti-Ty MAb showed that the protein migrated at approximately twice the size in nonreduced versus reduced conditions, demonstrating that MIC3ΔCBL is dimeric (Fig. 5A). In both conditions, MIC3ΔCBL appeared as a doublet, with the higher band corresponding to the immature form of the protein (Fig. 5B). SSP-CBL-E23 also appeared as a doublet. A lower apparent molecular size was observed in unreduced conditions, meaning that the difference probably was due to the reduction of internal disulfide bonds. Similar results were obtained for SSP-CBL-E2, except that the proprotein was not detected in the reduced condition (Fig. 5B). Therefore, and consistently with the absence of the dimerization domain in SSP-CBL-E2 and SSP-CBL-E23, our results indicated that SSP-CBL-E2 and SSP-CBL-E23 are monomeric proteins. An analysis of these proteins by IFA showed that SSP-CBL-E2 and SSP-CBL-E23 reached the micronemes (Fig. 4A). Taken together, these data provide evidence that targeting to micronemes does not require the dimerization of MIC3.

Unprocessed forms of MIC3 can reach the micronemes. We then analyzed the cleavage of propeptide in all of the modified MIC3 proteins that we have generated in *T. gondii* by Western blotting using anti-Ty and anti-propeptide Abs (Fig. 5B). The anti-Ty Ab could recognize both mature and immature forms of the recombinant proteins, whereas the anti-propeptide Ab revealed exclusively immature proteins. The processing of SSP-CBL could not be analyzed due to the low expression level of the protein. In MIC3ΔCBL, SSP-CBL-E23, and SSPE3, the anti-Ty Abs recognized two specific bands corresponding to (i) the immature form for the higher band, also revealed by the anti-propeptide serum, and (ii) the mature form for the lower band (not detected by anti-propeptide serum). The immature form was always less abundant. These results showed that MIC3ΔCBL, SSP-CBL-E23, and SSPE3 are correctly processed. SSP-CBL-E2 was poorly expressed, and only a faint single band was detected with anti-Ty, with an apparent molecular mass clearly lower than that of the band detected with the anti-propeptide, suggesting that the propeptide is cleaved in SSP-CBL-E2 but that the immature form is not abundant enough to be detected by the anti-Ty MAb. In SSPE2 and SSPE4, both anti-Ty and anti-propeptide serum detected a single band of identical M_rs, showing that in these two constructs the propeptide was not cleaved. Since SSPE2 and SSPE4 reached the micronemes (Fig. 4), our results show that unprocessed forms of MIC3 can reach the micronemes.

DISCUSSION

Invasion and intracellular multiplication in *T. gondii* involve a highly orchestrated system of regulated secretion pathways from three distinct organelles, called micronemes, rhoptries, and dense granules. The correct prepackaging of specific proteins in each compartment is a key step toward productive infection, but the mechanisms of protein targeting remain poorly defined. The present study underlines the multifactorial nature of microneme sorting. We have shown that two distinct elements in the MIC3 protein (the propeptide and an EGF domain) participate in microneme targeting, suggesting that multiple elements function in different steps in the microneme pathway.

To address the role of the propeptide in MIC3 trafficking, we generated MIC3ΔPro-expressing parasites and found that the propeptide was necessary for the efficient trafficking of MIC3 to the micronemes. A role for microneme propeptides in trafficking also is supported by a parallel study of the propeptides of M2AP and MIC5 (7, 20), other soluble *Toxoplasma* MICs (33), although the outcomes of MIC3ΔPro, M2APΔPro, and MIC5ΔPro proteins are completely different. MIC5ΔPro is retained in the ER-Golgi complex. The propeptide deletion in MIC3 resulted in delivery to the vacuolar space, probably via dense granules that constitute the default constitutive pathway for soluble proteins. In contrast, M2APΔPro is retained in the secretory pathway in an endosome-like compartment similar to that occupied by pro-M2AP, indicating that the transgenic MIC2-M2AP (TgMIC2-M2AP) complex traffics through the TGN and then through the early endosomes (20), a compartment that has been proposed as a basic sorting platform in higher eukaryotic cells (35). Micronemes, as suggested for rhoptries, may bud directly from this site (31). In M2AP, the propeptide would contain trafficking information to move the TgMIC2-M2AP complex beyond the early endosome to reach the micronemes. Interestingly, our study shows that the dele-

tion of tandemly repeated EGF2, EFG3, and EGF4 leads to the retention of the immature protein within the secretory pathway in a compartment analogous to that labeled by the anti-pro-M2AP. One possibility is that the propeptide of MIC3 would first act as a targeting signal to direct the protein to early endosomes, and then the information contained in the EGF sequences would direct the protein to micronemes or to an intermediate compartment corresponding to immature micronemes, where proteolytic maturation would occur. Any one of EGF2, EGF3, and EGF4 can fulfill such endosome-like-to-microneme trafficking, although they exhibit little sequence similarity (between 18 to 28% identity and 28 to 31% similarity). No consensus sequence has been deduced from the alignment of EGF2, EGF3, and EGF4, suggesting a possible conformation-dependent function. What mechanism operates in microneme sorting is unknown. In higher eukaryotic cells, the sorting of proteins toward constitutive versus regulated secretory pathways occurs in or after the TGN, and two hypotheses are proposed to account for the biogenesis of regulated secretory vesicles (15). In the first model, referred to as sorting by entry, sorting occurs through the action of a sorting receptor present in the TGN that traps proteins destined to secretory granules at the nascent-granule budding sites (11, 12). In the second model, referred to as sorting by retention, all secretory proteins are sorted into immature secretory granules, but proteins destined to the constitutive secretion pathway are removed by the budding of constitutive secretory vesicles containing nonaggregated proteins (4). Both models require that pro-MIC3 and EGF domains of MIC3 participate in the selective aggregation or specific receptor recognition. All attempts at coprecipitating tachyzoite proteins on a recombinant protein corresponding to the MIC3 propeptide have failed so far (M. Lebrun, unpublished data). In mammalian cells, short α-helix domains also may direct proteins to secretory granules, and Dikeakos et al. recently have demonstrated that the presence of charged (either positive or negative) amino acids spatially segregated from a hydrophobic patch in the α-helices of secretory proteins likely played a critical role in the ability of these structures to direct secretory granule sorting (14). An examination of the secondary structure of MIC3 by using all of the programs available on the EXPASY server (http://www.expasy.org/) did not reveal the presence of such peculiar structures in the propeptide and in the EGF domains.

A previous study aimed at identifying microneme-targeting signals in MIC3 suggested the presence of multiple targeting sequences without precisely delineating the domains involved (36). Here, we show that AA1-189 or AA1-236, which corresponds to SSP-CBL-E2 and SSP-CBL-E23 constructs, respectively, is targeted properly to micronemes, while Striepen et al. (36) showed that an intermediary construct (AA1-225) resulted in arrest within the secretory pathway. In this construct, a quarter of the EGF3 was arbitrarily truncated, so that this module contained five cysteines instead of six, which probably disturbed the formation of critical disulfide bonds, leading to the misfolding of the EGF-like domain and conformation-dependent retention in the ER-Golgi complex. Also, we showed here that SSP-CBL-$AA_{294\text{-}359}$ was retained in endosome-like structures, while Striepen et al. (36) showed that a construct in which the C-terminal domain (AA306-359) was fused directly downstream of the MIC3 signal peptide resulted in apparent microneme targeting. In addition, they showed that in the absence of the propeptide, some truncated constructs were arrested in the secretory pathway in a region anterior to the nucleus, although we show here that in the absence of propeptide, the protein is mistargeted to the PV. A plausible explanation for these differences comes from the fact that their work was performed with GFP-tagged transgenic MIC3 fragments expressed in wild-type parasites. Since MIC3 is a dimer, endogenous native MIC3 monomers may have interacted with the truncated forms of MIC3-GFP. Here, all constructs were generated in the *mic3* KO background to exclude such a possibility. This led us to identify more precisely the MIC3 sequence regions involved in targeting to micronemes.

Although we have established the involvement of the propeptide of MIC3 in trafficking, we do not know precisely where its proteolytic cleavage occurs. The generation of a MIC3 mutant that is expressed as an unprocessed form and retained in the secretory pathway (SSP-CBL-$AA_{294\text{-}359}$) indicates that the protease resides in a postendosomal compartment, similarly to that observed for M2AP and MIC5 (7, 20). Whether or not the same protease cleaves MIC3 and other MICs has yet to be analyzed. The cleavage sites of the two proteins are completely different (AQLS/TFLE for M2AP and SSVQ/SPSK for MIC3). The generation of individual or multiple cleavage site mutants in M2AP reveals that extensive mutations on both sides (P4 and P4′) of the cleavage site are required to generate cleavage resistance, indicating that the protease does not require a strict consensus for its activity (20). Individual and double substitutions around the MIC3 cleavage site also had no apparent effect on processing (M.L., unpublished). The precise role of propeptide processing in facilitating the entry of MIC3 into the microneme pathway remains to be delineated. However, we showed here that the processing of some of the MIC3 constructs (SSPE2 and SSPE4) is dispensable for their correct targeting, suggesting that, as for M2AP (20) and MIC5 (7), the processing event of MICs is not a prerequisite to their packaging in micronemes.

In previous studies, we have shown that the CBL domain of MIC3 is involved in the recognition of host receptor(s), probably via interaction with sugar moieties, and that the propeptide inhibits the receptor binding activity of the CBL domain (9). Our first interpretation was that the propeptide prevented the inappropriate association of MIC3 with other parasite proteins, in particular, glycosylated proteins transiting in the ER-Golgi complex. Our present data do not support this view, but rather show that the propeptide of MIC3 is needed for the proper targeting of the protein, and it may assist in the folding of the protein but must be eliminated to allow the expression of the adhesive property of the CBL domain.

In contrast to other MICs, a significant amount of MIC3 is retained in the secretory pathway upon synthesis. This is observed only during daughter separation or in newly split parasites. In addition, this material appears in a very narrow window of time, when MIC3 synthesis precedes that of other MIC proteins (as determined from our experiments with M2AP) and does not increase afterwards. Later on, MIC3 behaves similarly to M2AP, with both showing propeptide labeling in the endosome-like compartment in newly split parasites and the typical microneme staining in all other stages of the life

cycle. This unique behavior could reflect a partial misregulation of MIC3 expression with respect to its putative escort, probably related to a different timing of promoter activation. Interestingly, this phenomenon is not observed with the MIC3-GFP (36) that is expressed under a tubulin promoter (M.L., unpublished). The strong IFA signal of MIC3 retained in the ER contrasted with the much fainter signal in micronemes and leads us to conclude that most of the material observed in the ER does not exit and probably is degraded. A saturation of the sorting receptor that interacts directly or indirectly with MIC3 also could be proposed to explain this behavior of MIC3. In any case, the biological significance of this phenomenon remains elusive.

In mammalian cells, a plethora of signals that direct proteins to secretory granules have been identified, but no consensus signal exists, and more than one mechanism may exist depending on the cell and on the type of the protein. Our data further underline that microneme targeting in apicomplexa also is a multifactorial process involving the regulated coordination of multiple interactions. Further studies are needed to dissect the partners and compartments responsible for driving these major virulence factors to their sites of action.

ACKNOWLEDGMENTS

We thank Vern Carruthers and Con Beckers for the generous gifts of anti-pro-M2AP and anti-IMC1 Abs, respectively. We are grateful to Sebastien Besteiro for the critical review of the manuscript. We thank Veronique Richard for help with electron microscopy.

O.C. is a recipient of a fellowship from VIHPAL and Fondation pour la Recherche Médicale (FRM). This work was supported by CNRS and a grant from FRM to J.F.D.

REFERENCES

1. **Achbarou, A., O. Mercereau-Puijalon, J. M. Autheman, B. Fortier, D. Camus, and J. F. Dubremetz.** 1991. Characterization of microneme proteins of *Toxoplasma gondii*. Mol. Biochem. Parasitol. **47:**223-233.
2. **Alexander, D. L., J. Mital, G. E. Ward, P. Bradley, and J. C. Boothroyd.** 2005. Identification of the moving junction complex of *Toxoplasma gondii*: a collaboration between distinct secretory organelles. PLoS Pathog. **1:**e17.
3. **Appella, E., I. T. Weber, and F. Blasi.** 1988. Structure and function of epidermal growth factor-like regions in proteins. FEBS Lett. **231:**1–4.
4. **Arvan, P., and D. Castle.** 1998. Sorting and storage during secretory granule biogenesis: looking backward and looking forward. Biochem. J. **332:**593–610.
5. **Bastin, P., Z. Bagherzadeh, K. R. Matthews, and K. Gull.** 1996. A novel epitope tag system to study protein targeting and organelle biogenesis in *Trypanosoma brucei*. Mol. Biochem. Parasitol. **77:**235–239.
6. **Bermudes, D., J. F. Dubremetz, A. Achbarou, and K. A. Joiner.** 1994. Cloning of a cDNA encoding the dense granule protein GRA3 from *Toxoplasma gondii*. Mol. Biochem. Parasitol. **68:**247–257.
7. **Brydges, S. D., J. M. Harper, F. Parussini, I. Coppens, and V. B. Carruthers.** 2007. A transient forward targeting element for microneme regulated secretion in *Toxoplasma gondii*. Biol. Cell. **100:**253–264.
8. **Carruthers, V. B.** 2006. Proteolysis and *Toxoplasma* invasion. Int. J. Parasitol. **36:**595–600.
9. **Cérède, O., J. F. Dubremetz, D. Bout, and M. Lebrun.** 2002. The *Toxoplasma gondii* protein MIC3 requires propeptide cleavage and dimerization to function as adhesin. EMBO J. **21:**2526–2536.
10. **Cérède, O., J. F. Dubremetz, M. Soete, D. Deslee, H. Vial, D. Bout, and M. Lebrun.** 2005. Synergistic role of micronemal proteins in *Toxoplasma gondii* virulence. J. Exp. Med. **201:**453–463.
11. **Chung, K. N., P. Walter, G. W. Aponte, and H. P. Moore.** 1989. Molecular sorting in the secretory pathway. Science **243:**192–197.
12. **Cool, D. R., E. Normant, F. Shen, H. C. Chen, L. Pannell, Y. Zhang, and Y. P. Loh.** 1997. Carboxypeptidase E is a regulated secretory pathway sorting receptor: genetic obliteration leads to endocrine disorders in Cpe(fat) mice. Cell **88:**73–83.
13. **Di Cristina, M., R. Spaccapelo, D. Soldati, F. Bistoni, and A. Crisanti.** 2000. Two conserved amino acid motifs mediate protein targeting to the micronemes of the apicomplexan parasite *Toxoplasma gondii*. Mol. Cell. Biol. **20:**7332–7341.
14. **Dikeakos, J. D., M. J. Lacombe, C. Mercure, M. Mireuta, and T. L. Reudelhuber.** 2007. A hydrophobic patch in a charged alpha-helix is sufficient to target proteins to dense core secretory granules. J. Biol. Chem. **282:**1136–1143.
15. **Dikeakos, J. D., and T. L. Reudelhuber.** 2007. Sending proteins to dense core secretory granules: still a lot to sort out. J. Cell Biol. **177:**191–196.
16. **Donald, R. G., D. Carter, B. Ullman, and D. S. Roos.** 1996. Insertional tagging, cloning, and expression of the *Toxoplasma gondii* hypoxanthine-xanthine-guanine phosphoribosyltransferase gene. Use as a selectable marker for stable transformation. J. Biol. Chem. **271:**14010–14019.
17. **Dubremetz, J. F.** 2007. Rhoptries are major players in *Toxoplasma gondii* invasion and host cell interaction. Cell. Microbiol. **9:**841–848.
18. **Garcia-Réguet, N., M. Lebrun, M. N. Fourmaux, O. Mercereau-Puijalon, T. Mann, C. J. Beckers, B. Samyn, J. Van Beeumen, D. Bout, and J. F. Dubremetz.** 2000. The microneme protein MIC3 of *Toxoplasma gondii* is a secretory adhesin that binds to both the surface of the host cells and the surface of the parasite. Cell. Microbiol. **2:**353–364.
19. **Hager, K. M., B. Striepen, L. G. Tilney, and D. S. Roos.** 1999. The nuclear envelope serves as an intermediary between the ER and Golgi complex in the intracellular parasite *Toxoplasma gondii*. J. Cell Sci. **112:**2631–2638.
20. **Harper, J. M., M. H. Huynh, I. Coppens, F. Parussini, S. Moreno, and V. B. Carruthers.** 2006. A cleavable propeptide influences *Toxoplasma* infection by facilitating the trafficking and secretion of the TgMIC2-M2AP invasion complex. Mol. Biol. Cell **17:**4551–4563.
21. **Hoppe, H. C., H. M. Ngo, M. Yang, and K. A. Joiner.** 2000. Targeting to rhoptry organelles of *Toxoplasma gondii* involves evolutionarily conserved mechanisms. Nat. Cell Biol. **2:**449–456.
22. **Karsten, V., H. Qi, C. J. Beckers, A. Reddy, J. F. Dubremetz, P. Webster, and K. A. Joiner.** 1998. The protozoan parasite *Toxoplasma gondii* targets proteins to dense granules and the vacuolar space using both conserved and unusual mechanisms. J. Cell Biol. **141:**1323–1333.
23. **Keeley, A., and D. Soldati.** 2004. The glideosome: a molecular machine powering motility and host-cell invasion by apicomplexa. Trends Cell Biol. **14:**528–532.
24. **Klausner, R. D., J. G. Donaldson, and J. Lippincott-Schwartz.** 1992. Brefeldin A: insights into the control of membrane traffic and organelle structure. J. Cell Biol. **116:**1071–1080.
25. **Laemmli, U. K.** 1970. Cleavage of structural proteins during the assembly of the head of bacteriophage T4. Nature **227:**680–685.
26. **Lebrun, M., V. B. Carruthers, and M. F. Cesbron-Delauw.** 2007. *Toxoplasma* secretory proteins and their roles in cell invasion and intracellular survival, p. 265–307. *In* L. M. Weiss and K. Kim (ed.), *Toxoplasma gondii*: the model apicomplexan-perspectives and methods. Academic Press, New York, NY.
27. **Lebrun, M., A. Michelin, H. El Hajj, J. Poncet, P. J. Bradley, H. Vial, and J. F. Dubremetz.** 2005. The rhoptry neck protein RON4 relocalizes at the moving junction during *Toxoplasma gondii* invasion. Cell. Microbiol. **7:**1823–1833.
28. **Mann, T., E. Gaskins, and C. Beckers.** 2002. Proteolytic processing of TgIMC1 during maturation of the membrane skeleton of *Toxoplasma gondii*. J. Biol. Chem. **277:**41240–41246.
29. **Meissner, M., M. Reiss, N. Viebig, V. B. Carruthers, C. Toursel, S. Tomavo, J. W. Ajioka, and D. Soldati.** 2002. A family of transmembrane microneme proteins of *Toxoplasma gondii* contain EGF-like domains and function as escorters. J. Cell Sci. **115:**563–574.
30. **Mercier, C., K. D. Adjogble, W. Daubener, and M. F. Delauw.** 2005. Dense granules: are they key organelles to help understand the parasitophorous vacuole of all apicomplexa parasites? Int. J. Parasitol. **35:**829–849.
31. **Ngô, H. M., M. Yang, K. Paprotka, M. Pypaert, H. Hoppe, and K. A. Joiner.** 2003. AP-1 in *Toxoplasma gondii* mediates biogenesis of the rhoptry secretory organelle from a post-Golgi compartment. J. Biol. Chem. **278:**5343–5352.
32. **Pelletier, L., C. A. Stern, M. Pypaert, D. Sheff, H. M. Ngo, N. Roper, C. Y. He, K. Hu, D. Toomre, I. Coppens, D. S. Roos, K. A. Joiner, and G. Warren.** 2002. Golgi biogenesis in *Toxoplasma gondii*. Nature **418:**548–552.
33. **Rabenau, K. E., A. Sohrabi, A. Tripathy, C. Reitter, J. W. Ajioka, F. M. Tomley, and V. B. Carruthers.** 2001. TgM2AP participates in *Toxoplasma gondii* invasion of host cells and is tightly associated with the adhesive protein TgMIC2. Mol. Microbiol. **41:**537–547.
34. **Reiss, M., N. Viebig, S. Brecht, M. N. Fourmaux, M. Soete, M. Di Cristina, J. F. Dubremetz, and D. Soldati.** 2001. Identification and characterization of an escorter for two secretory adhesins in *Toxoplasma gondii*. J. Cell Biol. **152:**563–578.
35. **Rodriguez-Boulan, E., and A. Musch.** 2005. Protein sorting in the Golgi complex: shifting paradigms. Biochim. Biophys. Acta **1744:**455–464.
36. **Striepen, B., D. Soldati, N. Garcia-Reguet, J. F. Dubremetz, and D. S. Roos.** 2001. Targeting of soluble proteins to the rhoptries and micronemes in *Toxoplasma gondii*. Mol. Biochem. Parasitol. **113:**45–53.